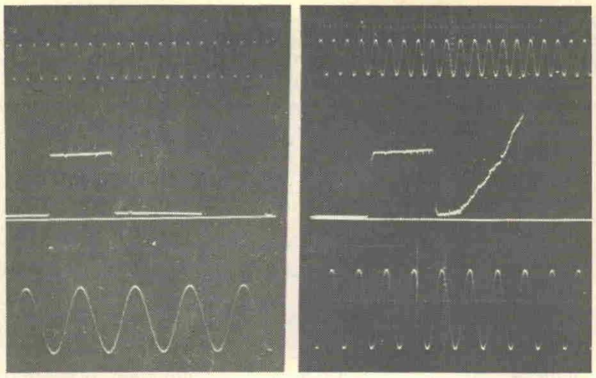

(a) (b)

FIG. 3. Typical current-time responses of x-cut quartz gauges subjected to short-duration stress pulses include those loaded below the threshold for anomalous response (a) and those loaded above the threshold of anomalous response (b). For both records, time increases from left to right. The response shown in (a) is normal in all respects; the current jumps to a value upon impact and falls to zero upon unloading. Even though the record in (b) shows a normal response until unloading occurs, a large positive excursion of current is observed late in time when the stress at the input electrode is zero. The transit time for these records is 1.11 μsec and the relative pulse durations are both 0.41. The stress applied is 9.42 kbar in (a) and 19.0 kbar in (b). Timing and voltage calibrations are shown above and below the signal traces.

Considerable care was used in the construction and inspection of each sample gauge used in the present investigation. The gauges were constructed with nominal specifications as previously given[6]; however, improved fabrication techniques[14] permitted improved performance. The guard-ring configuration was sandblasted into the plus x electrode of the quartz disk and inspected both optically and electrically. The electrode on the impact face was temporatily removed so that each disk could be inspected for inclusions in the quartz disk. Acmite inclusions[19] were found to be excessive in many disks; however, all disks used in these experiments were selected for low acmite concentrations. The open-face inspection also permitted examination of the solder connection to the rear electrode for signs of cracking due to thermal stresses. The bond of the Epoxy to the lateral surfaces and to the insulating gap was also inspected through the open face. After inspection and assembly, the impact-face electrode was vapor plated with aluminum.

Impact alignment was controlled by rigidly and precisely controlling all tolerances which can lead to misalignment. The flier is attached to the projectile with a perpendicularity of less than 50 μrad. The 28-cm-long projectile is fit to the bore of the barrel to within 2.5×10^{-3} cm on the diameter. The alignment flange on the muzzle is lapped flat and is perpendicular to the bore to within 30 μrad. The perpendicularity and parallelism of the specimen and projectile are measured for each experiment. The alignment flange is lapped frequently and the surface kept under careful scrutiny for minute damage. More details of these alignment control techniques are given in a recent publication.[14]

The current pulses from the gauges were recorded on Tektronix 585 or 454 oscilloscopes. Air dielectric cable, $\frac{7}{8}$ in. in diameter, is used for signal transmission from the gauge to the oscilloscope. The electrical impedances of cables, connectors, and terminators were checked for equivalence with a time-domain reflectometer. A newly developed pulse calibrator was used in the later part of the investigation. Important details of this instrumentation are also given in our recent publication.[14]

III. RESULTS

Two typical current-vs-time records obtained from shock-loaded sample gauges are shown in Fig. 3. Both experiments were conducted with the same flier and gauge thicknesses. The record at the lower stress, Fig. 3(a), is normal in all respects and corresponds with that expected from Eq. (1). On the other hand, the record at the higher stress shows a pronounced anomalous tail which cannot be predicted from Eq. (1) but has been found to be typical of responses well above an input stress threshold. The existence of an input stress threshold for the anomalous response can be deduced from these two experiments; however, determination of the precise value for this threshold requires more data in which both stress and pulse duration T_0 are varied in the immediate neighborhood of the threshold. Accordingly, the input stress threshold for anomalous response was investigated at six different pulse durations with impact configurations as tabulated in Table I. Experiments involving long pulse duration, i.e., $T_0 > t_0$, were also conducted on $-x$ orientation disks when similarities were discovered between the previously investigated[5–9] "$-x$ anomaly" and the present "short-pulse anomaly."

Table I includes nominal values for the relative pulse duration $\overline{T}_0/t_0 = 2l_f/l_t$, where $\overline{T}_0$ is the time for the stress pulse to complete a round trip through the unstressed thickness l_f of the flier and t_0 is the one-way transit time through the unstressed sample thickness l_t. Although these values are correct to a few percent, the exact values for the relative pulse durations depend upon the exact values of thickness and to a secondary extent upon the particle velocities and the loading and unloading wave velocities in quartz.

TABLE I. Summary of impact configurations.

Configuration	Flier thickness (mm)	Gauge thickness (mm)	Relative pulse duration $\overline{T}_0/t_0$—nominal
A	0.65	8.58	0.152
B	0.65	6.35	0.205
C	1.31	8.58	0.305
D	1.31	6.35	0.413
E	1.94	6.35	0.611
F	2.56	6.35	0.806
G	>6.4	6.35[a]	>1.0

[a] The gauges in configuration G were constructed in the $-x$ orientation, i.e., the guard ring was constructed in the $-x$ electrode and the impact occurred on the $+x$ electrode.

TABLE II. Summary of experiments.

Shot No.	T_0/t_s	Tilt (μrad)	u^a (mm/μsec)	σ^b (kbar)	Response
532	0.152	260	0.1883	28.5	small anomaly
529	0.152	90	0.1925	29.2	anomaly
476	0.205	1960	0.1314	19.9	normal
478	0.205	5850	0.1555	23.6	normal
477	0.205	920	0.1668	25.3	small anomaly
490	0.308	770	0.0975	14.8	very small anomaly
488	0.310	870	0.1102	16.7	anomaly
487	0.307	1030	0.1187	18.0	anomaly
430	0.412	150	0.0622	9.42	normal
475	0.413	425	0.0894	13.5	very small anomaly
462	0.414	470	0.1018	15.4	small anomaly
460	0.415	380	0.1119	17.0	anomaly
431	0.415	550	0.1257	19.0	anomaly
483	0.418	1180	0.1666	25.3	anomaly
528	0.612	220	0.0761	11.5	anomaly
464	0.614	820	0.0783	11.9	normal
479	0.614	450	0.0900	13.6	anomaly
465	0.616	940	0.0981	14.9	anomaly
511	0.813	315	0.0662	10.0	normal
513	0.814	280	0.0708	10.7	anomaly
512	0.815	320	0.0800	12.1	anomaly
thick fliers, $-x$ orientation					
463	>1.0	75	0.0685	10.4	normal
486	>1.0	450	0.0711	10.8	anomaly
473	>1.0	120	0.0736	11.2	anomaly
618	>1.0	385	0.1016	15.4	anomaly

[a] u is the input particle velocity taken as $\frac{1}{2}$ the measured impact velocity.

[b] σ is the input stress computed from the conservation of momentum relation $\sigma=\rho_0 U u$. ρ_0 is 2.65 g cm^{-3} and U is 5.72 mm/μsec.

A. Pulse Durations and Wave Velocity

Upon impact, shock waves are imparted into both the sample disk and the flier. The duration of the stress pulse imparted to the sample is controlled by the round-trip transit time of the shock wave through the flier. Since surfaces of the flier and sample are either stationary or move with the particle velocity amplitudes, the thicknesses of the disks change in time until unloading is completed. Furthermore, the transit times depend upon the velocities of both the loading and unloading wave fronts. To calculate the pulse duration and sample thicknesses after unloading, both the loading and unloading shock fronts are assumed to travel with a velocity in laboratory coordinates, U, that is independent of stress. Under this condition, $T_0 = 2l_f/U$ and the transit time through the stressed sample after unloading t_s is

$$t_s = t_0\left(1 - \frac{u}{U}\frac{T_0}{t_0}\right). \tag{3}$$

Since the maximum value of u/U employed in this investigation is 0.034, the nominal values of T_0/t_0 are very close to the values of T_0/t_s.

The shock velocities of the wave fronts must be determined experimentally. Previous measurements have indicated that the shock velocity of x-cut quartz has a constant value to within ±1% up to a stress of 25 kbar. Unloading wave velocities have not previously been measured, however, and a small increase in wave velocity in compression will cause a larger change to the unloading wave dispersion and influence the unloading wave shape. The present experiments afford the opportunity to test the unloading wave velocity by measuring differences between the loading time and the unloading time indicated on the current-time records. If the shock velocity is dependent on stress, the unloading stress pulse will disperse or "shock up" depending on the curvature of the stress-volume relation. To the time resolution of the present measurements, about 5 nsec, there was no evidence for dispersion or "shocking up" in the loading and unloading times indicated on the experimental records. Thus, in confirmation of previous observations, the shock velocity is independent of stress values up to 25 kbar and the shock speed equals the adiabatic sound speed. The present observation gives confirmation to the constant wave velocity to an accuracy of $\pm\frac{1}{2}\%$.

B. Threshold for Anomalous Response

A detailed tabulation of values determined in each experiment is shown in Table II. The principal observation is the existence or nonexistence of the anomalous tail for various values of stress and relative pulse duration. The experimental conditions were chosen to investigate the immediate neighborhood of the threshold for six different pulse durations with input stresses both above and below the threshold zone.

The locations where experiments were conducted in the relative-pulse-duration vs input-stress plane are dis-